

## Article

# LRIF1 interacts with HP1 $\alpha$ to coordinate accurate chromosome segregation during mitosis

Saima Akram<sup>1,†</sup>, Fengrui Yang<sup>1,2,†</sup>, Junying Li<sup>1,†</sup>, Gregory Adams<sup>2,3</sup>, Yingying Liu<sup>1,2</sup>, Xiaoxuan Zhuang<sup>1,3</sup>, Lingluo Chu<sup>4</sup>, Xu Liu<sup>1,2</sup>, Nerimah Emmett<sup>2</sup>, Winston Thompson<sup>2</sup>, McKay Mullen<sup>2</sup>, Saravana Muthusamy<sup>2</sup>, Wenwen Wang<sup>1,2</sup>, Fei Mo<sup>1,3,\*</sup>, and Xing Liu<sup>1,2,\*</sup>

<sup>1</sup> Anhui Key Laboratory for Cellular Dynamics, University of Science & Technology of China School of Life Sciences, National Science Center for Physical Sciences at Nanoscale, and Chinese Academy of Science Center of Excellence on Molecular Cell Sciences, Hefei 230027, China

<sup>2</sup> Keck Center for Molecular Imaging, Department of Physiology, Morehouse School of Medicine, Atlanta, GA 30310, USA

<sup>3</sup> National Institutes of Health, Bethesda, MD 20892, USA

<sup>4</sup> Department of Molecular Cell Biology, Harvard University, Cambridge, MA 02138, USA

<sup>†</sup> These authors contributed equally to this work.

\* Correspondence to: Fei Mo, E-mail: fei.mo@nih.gov; Xing Liu, E-mail: xing1017@ustc.edu.cn

Edited by Zhiyuan Shen

**Heterochromatin protein 1 $\alpha$  (HP1 $\alpha$ ) regulates chromatin specification and plasticity during cell fate decision. Different structural determinants account for HP1 $\alpha$  localization and function during cell division cycle. Our earlier study showed that centromeric localization of HP1 $\alpha$  depends on the epigenetic mark H3K9me3 in interphase, while its centromeric location in mitosis relies on uncharacterized PXVXL-containing factors. Here, we identified a PXVXL-containing protein, ligand-dependent nuclear receptor-interacting factor 1 (LRIF1), which recruits HP1 $\alpha$  to the centromere of mitotic chromosomes and its interaction with HP1 $\alpha$  is essential for accurate chromosome segregation during mitosis. LRIF1 interacts directly with HP1 $\alpha$  chromoshadow domain via an evolutionarily conserved PXVXL motif within its C-terminus. Importantly, the LRIF1–HP1 $\alpha$  interaction is critical for Aurora B activity in the inner centromere. Mutation of PXVXL motif of LRIF1 leads to defects in HP1 $\alpha$  centromere targeting and aberrant chromosome segregation. These findings reveal a previously unrecognized direct link between LRIF1 and HP1 $\alpha$  in centromere plasticity control and illustrate the critical role of LRIF1–HP1 $\alpha$  interaction in orchestrating accurate cell division.**

**Keywords:** HP1 $\alpha$ , LRIF1, mitosis, centromere, chromosome segregation

## Introduction

Mitosis is the most dramatic orchestra of cell cycle that requires error-free distribution of genetic materials from parents to genetically identical daughter cells. The kinetochore is a supermolecular complex assembled at each centromere in eukaryotic cells, which provides a chromosomal attachment point for spindle microtubules and guarantees accurate movements of chromosomes during mitosis. While accurate chromosome segregation is essential for cell plasticity, aberrant mitosis contributes to tumorigenesis (Cleveland et al., 2003; Champion et al., 2017). Moreover, genomic stability and error-free chromosome segregation depend on accurate attachment, positioning, and biorientation of kinetochores with spindle microtubules (Rajagopalan and Lengauer, 2004; Shen, 2011; Patel et al., 2016).

Heterochromatin protein 1 homolog alpha (HP1 $\alpha$ ) is a multi-functional protein functions in various biological processes such as heterochromatin formation (Cheutin et al., 2003; Al-Sady et al., 2013; Canzio et al., 2013; Chu et al., 2014; Liu et al., 2014), transcriptional regulation (Kwon et al., 2010; Studencka et al., 2012), RNA interference (Rougemaille et al., 2012; Juang et al., 2013), DNA recombination and damage repair (Ball and Yokomori, 2009; Luijsterburg et al., 2009; Baldeyron et al., 2011), chromatin condensation (Verschure et al., 2005), centromere/kinetochore protein assembly (Obuse et al., 2004), and regulation of sister chromatid cohesion (Nonaka et al., 2002; Inoue et al., 2008; Yamagishi et al., 2008; Shimura et al., 2011). Although cell cycle-dependent association of HP1 $\alpha$  with chromatin has been characterized, recent studies showed that HP1 $\alpha$  function is regulated by its interacting proteins and post-translational modifications (Larson et al., 2017; Strom et al., 2017). Particularly, centromere localization of HP1 $\alpha$  during interphase depends on its chromodomain, while in mitosis, chromoshadow (CS) domain plays an essential role

Received December 29, 2017. Revised May 5, 2018. Accepted July 14, 2018.

© The Author(s) (2018). Published by Oxford University Press on behalf of *Journal of Molecular Cell Biology*, IBCB, SIBS, CAS. All rights reserved.

(Hayakawa et al., 2003; Chu et al., 2014). Furthermore, the chromodomain reads epigenetic mark H3K9me3 and recruits HP1 $\alpha$  to chromatin (Higgins and Prendergast, 2016), while CS domain is responsible for HP1 $\alpha$  dimerization and binding to PXVXL-containing ligands like INCENP and thus facilitates the recruitment of additional proteins to heterochromatin (Kiyomitsu et al., 2010; Kang et al., 2011; Higgins and Prendergast, 2016). During mitosis, phosphorylation of histone H3 Ser10 (pS10-H3) by Aurora B kinase dissociates HP1 $\alpha$  from the chromatin and relocates to the centromere (Fischle et al., 2005; Hirota et al., 2005; Chu et al., 2014). Our previous study revealed that inner centromere protein borealin directly interacts with HP1 $\alpha$  via an evolutionarily conserved PXVXL motif in the C-terminal borealin, which binds to the CS domain of HP1 $\alpha$  (Liu et al., 2014). This borealin–HP1 $\alpha$  interaction facilitates recruitment of the chromosomal passenger complex (CPC) to centromere and sustains Aurora B kinase activity in centromere.

Ligand-dependent nuclear receptor-interacting factor 1 (LRIF1), also known as C1orf103, was originally identified as a novel nuclear receptor co-repressor that associates with the nuclear matrix and named as RIF-1 (Li et al., 2007). In a proteome-wide search for HP1 $\alpha$  binding proteins, LRIF1 was also identified and named as HBiX1 based on its role in X chromosome inactivation (Nozawa et al., 2010). Conserved among vertebrates, LRIF1 contains an HP1-binding motif and a nuclear localizing signal (Li et al., 2007; Nozawa et al., 2013). However, the functional relevance of LRIF1–HP1 $\alpha$  interaction during cell cycle progression and how LRIF1 functions in cell division remain unknown.

To explore the molecular mechanism underlying HP1 $\alpha$  functional regulation, we screened for HP1 $\alpha$  binding proteins during mitosis and identified LRIF1 as an important functional partner of HP1 $\alpha$ . LRIF1 specifies the localization of HP1 $\alpha$  to centromere via its PXVXL motif in the C-terminus. Depletion of LRIF1 perturbs the centromere localization of HP1 $\alpha$ , which leads to erroneous cell division. Moreover, disruption of LRIF1–HP1 $\alpha$  interaction by a membrane-permeable competing peptide results in chromosome mis-segregation, demonstrating that LRIF1–HP1 $\alpha$  interaction plays an essential role in regulating mitotic progression.

## Results

### *Identification and characterization of HP1 $\alpha$ –LRIF1 interaction*

Our previous studies have revealed that the centromeric localization of HP1 $\alpha$  is determined by its chromodomain via interacting with H3K9me3 during interphase. In mitotic cells, the CS domain binds to PXVXL motif-containing proteins at the centromere (Chu et al., 2014). However, it remained elusive as how PXVXL motif-containing proteins specify the localization and function of HP1 $\alpha$  during mitosis. To characterize centromeric proteins interacting with HP1 $\alpha$  in mitosis, we immunoprecipitated HP1 $\alpha$ -containing protein complex from mitotic HeLa cell lysates and analyzed its composition by mass spectrometry as described previously (Fang et al., 2006; Huang et al., 2012). The screen identified LRIF1, which contains a conserved PXVXL motif (Leu-Arg-Val-Cys-Leu, Supplementary Figure S1A) and expressed both in interphase and mitosis (Supplementary Figure S1B). To validate LRIF1–HP1 $\alpha$

interaction, both interphase (I, thymidine-synchronized) and mitotic (M, nocodazole-synchronized) HeLa cells were harvested for immunoprecipitation, which indicated that LRIF1 interacts with HP1 $\alpha$  during both interphase and mitosis (Figure 1A and Supplementary Figure S1C).

To further characterize the physical interaction between LRIF1 and HP1 $\alpha$ , we generated multiple LRIF1 deletions and LRVCL motif mutants, assuming which could block the HP1 $\alpha$ –LRIF1 interaction, to pinpoint the binding domain of HP1 $\alpha$  on LRIF1 (Figure 1B). Consistent with our prediction, co-immunoprecipitation experiments confirmed that both the C-terminal of LRIF1 and the LRVCL motif are required for the interaction between LRIF1 and HP1 $\alpha$  (Supplementary Figure S1D and E). Furthermore, pull-down analysis indicated that the C-terminal of LRIF1 contributes to its association with HP1 $\alpha$  and mutation of LRVCL motif disrupted LRIF1–HP1 $\alpha$  interaction (Figure 1C). Thus, we conclude that HP1 $\alpha$  physically interacts with LRIF1 and the LRVCL motif is essential for the interaction.

### *LRIF1 is essential for faithful chromosome segregation during mitosis*

Although the role of HP1 $\alpha$  in mitosis is well documented, the function of LRIF1 in mitosis is unknown. To demonstrate the role of LRIF1 during mitosis, we first characterized the temporal dynamics of LRIF1 protein levels during mitosis by collecting synchronized HeLa cells at indicated intervals after releasing from the G1/S phase blocking. Interestingly, LRIF1 is slightly enriched in mitosis, indicating that LRIF1 expression is partially cell cycle-related (Supplementary Figure S2A). To further characterize the role of LRIF1, we employed siRNA to suppress endogenous LRIF1 and examined the loss-of-function of LRIF1 by time-lapse microscopy. As expected, siRNA targeting LRIF1 greatly suppressed the LRIF1 protein level (Supplementary Figure S2B). To evaluate the functional relevance of LRIF1 in chromosome segregation, time-lapse analysis was performed on LRIF1-suppressed cells. While control siRNA-transfected cells progressed through mitosis normally, TIP60 or LRIF1-depleted cells exhibited significant higher frequency of chromosome segregation defects (Figure 2A). These LRIF1-deficient cells exhibited mitotic arrest which appeared as unaligned chromosomes and premature anaphase with chromosome bridges as indicated in the magnified montage (Figure 2A). Quantitative analyses of mitotic cells from three independent experiments indicated that LRIF1 was essential for faithful mitotic progression (Figure 2B–E). This LRIF1-deficient elicited mitotic abnormality was further confirmed by the introduction of another LRIF1 siRNA (siRNA-2) (Supplementary Figure S2C–E). As shown in Supplementary Figure S2C, suppression of LRIF1 by the second siRNA resulted in premature anaphase with chromosome bridges in a similar fashion to that of the first siRNA. Thus, we confirmed that LRIF1 is essential for chromosome alignment and accurate metaphase–anaphase transition.

### *LRIF1 resides at centromere and colocalizes with HP1 $\alpha$ during mitosis*

To delineate the mechanism of action underlying LRIF1 function in mitosis, we examined the subcellular localization of

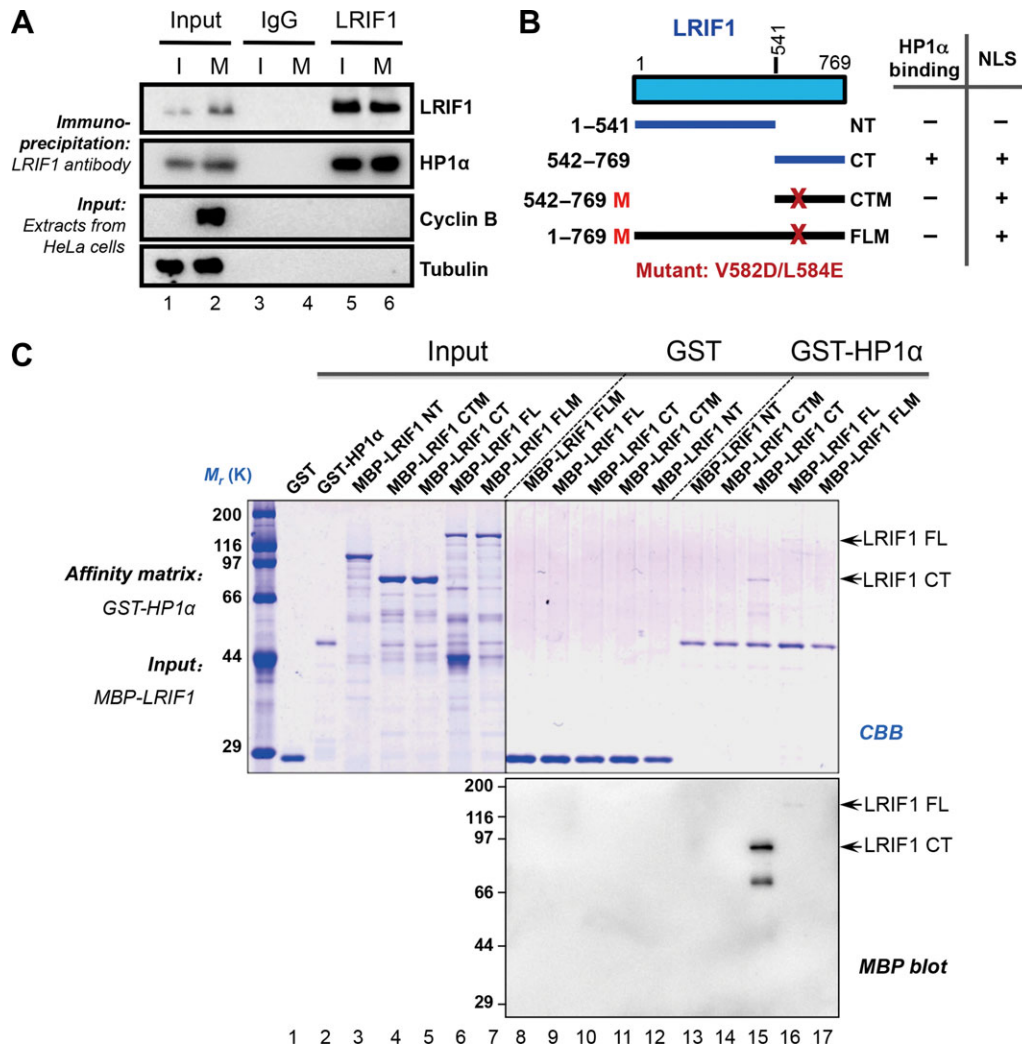


**Figure 1** LRIF1 is a novel interacting partner of HP1 $\alpha$  protein. **(A)** Thymidine-synchronized interphase HeLa cells (I) or nocodazole-treated mitotic HeLa cells (M) were extracted with Triton X-100-containing buffer. Clarified cell lysates were subjected to immunoprecipitation with LRIF1 antibody and control rabbit IgG, and separated by SDS-PAGE followed by western blotting with corresponding antibodies. Note that LRIF1 immunoprecipitation (IP) brought down HP1 $\alpha$  (lane 5 and 6). **(B)** Schematic drawing of LRIF1 truncation mutants. **(C)** GST-HP1 $\alpha$  recombinant protein on glutathione-agarose was used as an affinity matrix to absorb MBP-tagged LRIF1 and its deletion mutants. Samples were fractionated by SDS-PAGE, followed by Coomassie Brilliant Blue (CBB) staining (top panel). Western blotting using an anti-MBP antibody confirmed that both full-length (FL) and C-terminal (CT) LRIF1 proteins directly bound to HP1 $\alpha$  (bottom panel).

LRIF1 in mitotic HeLa cells. Our trial immunofluorescence study revealed that LRIF1 exhibits a typical deposition reminiscent of centromere and chromosome arms in multiple stages of mitosis (Supplementary Figure S3A), which is consistent with a pivotal role of LRIF1 in mitotic progression. To determine the precise localization of LRIF1 on chromosomal structures, we employed chromosome spread assay in which mitotic chromosomes were centrifugated onto a coverslip followed by immunostaining of LRIF1. As shown in Figure 3A (top panel), LRIF1 is located to the structure marked by anti-centromere antibody (ACA), in addition to chromosomal arms deposition. As expected, this specific centromere-associated

LRIF1 signal diminished in LRIF1 siRNA-transfected cells (Figure 3A and B).

To characterize the colocalization of LRIF1 with other mitotic kinetochore components, squashed chromosomes were stained for ACA, Hec1, LRIF1, and DAPI followed by examination under immunofluorescence microscopy. As shown in Figure 3C, the signals from ACA, Hec1, and LRIF1 were largely overlaid. Enlarged montages show a typical separated double-dot labeling from all three channels labeled with ACA, Hec1 and LRIF1. The line scan of the fluorescence intensity profiles further confirmed that the localization of LRIF1 is super-imposed with that of Hec1 at the outer kinetochores of chromosomes (Figure 3D).

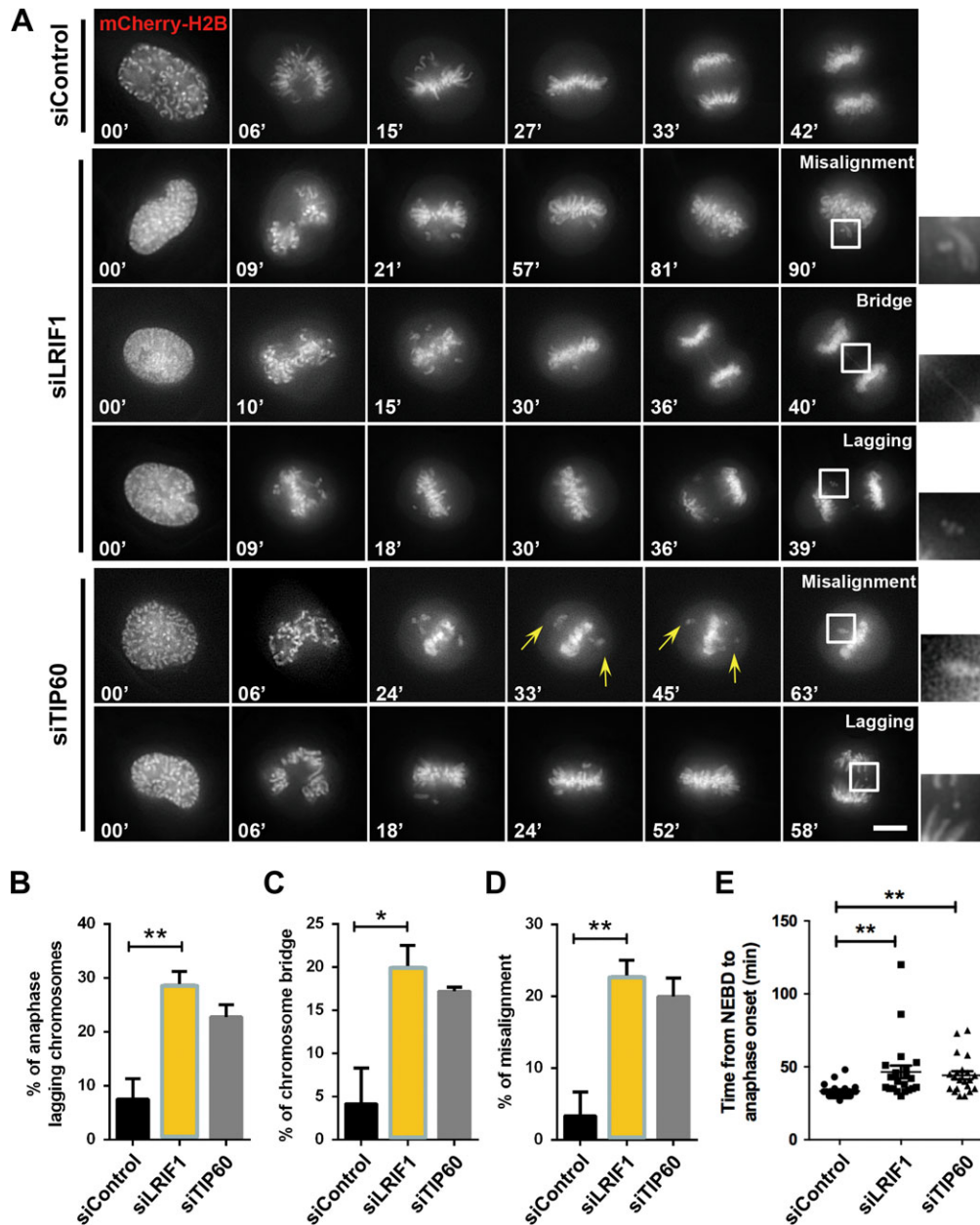


**Figure 2** LRF1 is required for accurate chromosome segregation in mitosis. **(A)** HeLa cells were transfected with LRF1 siRNA, TIP60 siRNA (as a positive control), or negative control siRNA and mCherry-H2B for live cell imaging. Representative phenotypes were shown. Scale bar, 10  $\mu$ m. **(B–E)** Quantification of mitotic phenotypes in **A**. Cells exhibiting unaligned chromosomes and failing to align at the metaphase plate within 60 min after nuclear envelope breakdown (NEBD) were considered to be misaligned. Scatter plot of the time from NEBD to anaphase onset was shown. At least 26 cells per group ( $n = 26$ , control siRNA;  $n = 35$ , LRF1 siRNA;  $n = 35$ , TIP60 siRNA) were examined from three independent experiments. Data represent mean  $\pm$  SEM and statistical significance was tested by two-sided *t*-test and represented by asterisks corresponding to  $*P < 0.05$ ,  $**P < 0.01$ .

Since we have confirmed the interaction between LRF1 and HP1 $\alpha$  in mitosis, we next sought to examine the colocalization of LRF1 and HP1 $\alpha$ . Using chromosome spreads from mitotic HeLa cells, it is apparent that HP1 $\alpha$  and LRF1 also colocalized to the centromere. In addition, a large fraction of HP1 $\alpha$  and LRF1 is located to chromosome arms as indicated in the

magnified montage (Figure 3E). To ascertain the dependence of LRF1 at kinetochore localization on spindle assembly checkpoint (SAC), mitotic cells were treated with reversine, an Mps1 inhibitor, before chromosome spread. As shown in Supplementary Figure S3B, reversine treatment dissociated Mad1 from kinetochores. However, LRF1 signal at the ACA-marked structure is not

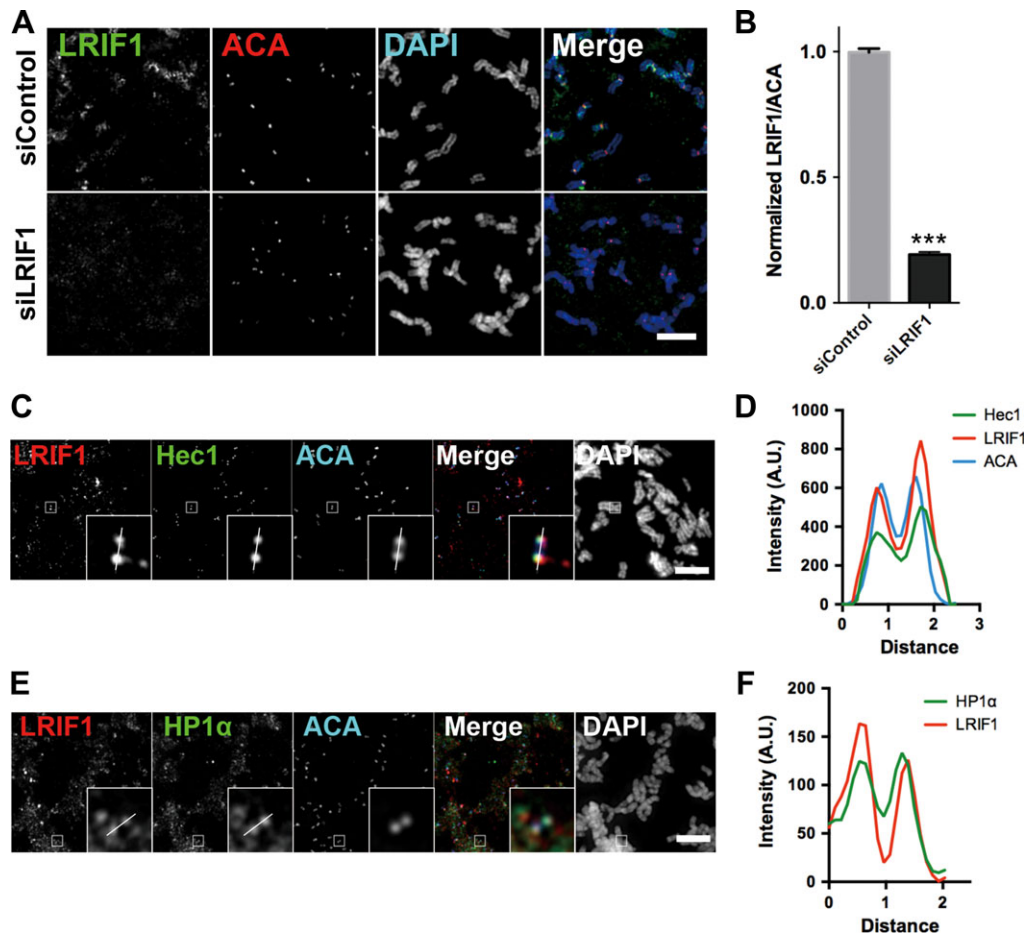


**Figure 3** LRIF1 colocalizes with HP1 $\alpha$  at centromere in mitosis. **(A)** HeLa cells were transfected with LRIF1 siRNA and synchronized with nocodazole followed by chromosome spread, fixation, and immunofluorescence staining. Scale bar, 10  $\mu$ m. **(B)** Quantification of LRIF1 fluorescence intensity (normalized to ACA) at kinetochores in LRIF1-depleted cells. Data represent mean  $\pm$  SEM and were examined with two-sided *t*-test. A total of 50 kinetochores were examined from three independent experiments. \*\*\**P* < 0.001. **(C)** HeLa cells were synchronized with nocodazole followed by chromosome spread, fixation, and immunofluorescence staining with antibodies of LRIF1 (red), Hec1 (green), and ACA (blue). Scale bar, 10  $\mu$ m. **(D)** Plot profile of LRIF1, ACA, and Hec1 fluorescence intensity across the kinetochore pair. **(E)** HeLa cells were synchronized with nocodazole followed by chromosome spread, fixation, and immunofluorescence staining with antibodies of LRIF1 (red), HP1 $\alpha$  (green), and ACA (blue). Scale bar, 10  $\mu$ m. **(F)** Plot profile of LRIF1 and HP1 $\alpha$  fluorescence intensity across the kinetochore pair.

abrogated (Supplementary Figure S3B, bottom panel). Our quantitative analyses confirmed that LRIF1 localization is independent of SAC activity (Supplementary Figure S3C and D). Thus, we conclude that LRIF1 is a *bona fide* component of centromere and LRIF1-HP1 $\alpha$  is a novel complex that resides at centromere during mitosis.

#### LRIF1-HP1 $\alpha$ interaction is essential for accurate mitosis

To explore the functional relevance of LRIF1-HP1 $\alpha$  interaction in mitosis, HeLa cells were transiently transfected to express wild-type GFP-LRIF1 and HP1 $\alpha$  binding-deficient GFP-LRIF1 FLM together with mCherry-H2B in the absence of endogenous LRIF1 protein followed by real-time analyses. As shown in Figure 4A, full-length GFP-LRIF1-expressing HeLa cells successfully completed cell division, while GFP-LRIF1 FLM-expressing cells

exhibited severe chromosome mis-segregation phenotype such as transient lagging chromosomes and delayed metaphase alignment followed by premature anaphase with chromosome bridge (Figure 4A, arrows). Statistical analyses show that expression of GFP-LRIF1 FLM increased the rate of chromosomal abnormalities in mitosis (Figure 4B). As shown in Figure 4C, the expression of GFP-LRIF1 FLM extended the intervals from the NEBD to anaphase onset (*P* < 0.05), indicating that LRIF1 is essential for accurate chromosome segregation and checkpoint satisfaction. Interestingly, GFP-LRIF1 FLM exhibits reduced centromere localization during live mitosis (Supplementary Figure S4A and B).

To assess the precise function of LRIF1-HP1 $\alpha$  interaction in mitotic chromosome movements, we fused the membrane-permeable TAT protein transduction motif with amino acids 565-600 of LRIF1 and GFP protein, named TAT-GFP-LRIF1<sup>A</sup>, which

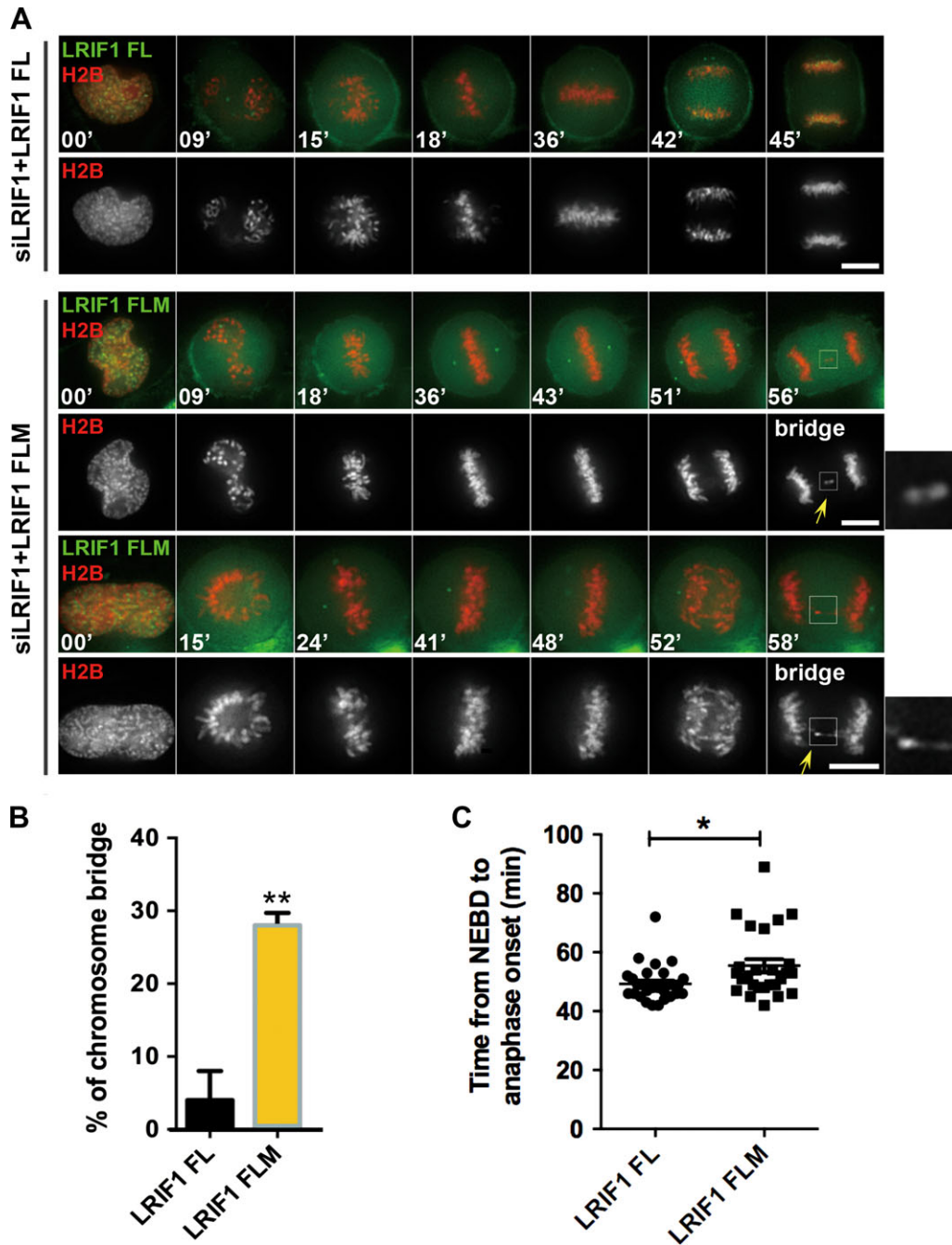


**Figure 4** LRIF1–HP1 $\alpha$  interaction is essential for accurate mitosis. **(A)** Real-time imaging of chromosome movement in cells expressing LRIF1 siRNA and RNAi-resistant GFP-LRIF1 FL (full-length) or its mutant GFP-LRIF1 FLM (full-length mutant). To visualize chromosome movement with a DeltaVision system, cells were co-transfected with mCherry-H2B. Scale bar, 10  $\mu$ m. **(B)** Statistical analysis of chromosome bridges in **A**. At least 26 cells per group ( $n = 30$ , LRIF1 FL;  $n = 26$ , LRIF1 FLM) were examined from three independent experiments. **(C)** Statistical analysis of mitotic delay judged by the intervals between NEBD and anaphase onset in **A** ( $n = 30$ , LRIF1 FL;  $n = 26$ , LRIF1 FLM). Data represent mean  $\pm$  SEM and statistical significance was tested by two-sided  $t$ -test and represented by asterisks corresponding to  $*P < 0.05$ ,  $**P < 0.01$ .

could compete with endogenous LRIF1 for HP1 $\alpha$  binding (Figure 5A). As expected, the recombinant TAT-GFP-LRIF1 $\Delta$  competed with endogenous LRIF1 and therefore disrupted the LRIF1–HP1 $\alpha$  association (Figure 5B, lane 5). As a negative

control, TAT-GFP protein did not interfere with the interaction between LRIF1 and HP1 $\alpha$  (Figure 5B, lane 4).

To determine whether the LRIF1–HP1 $\alpha$  interaction is required for mitotic progression, cells expressing mCherry-H2B were

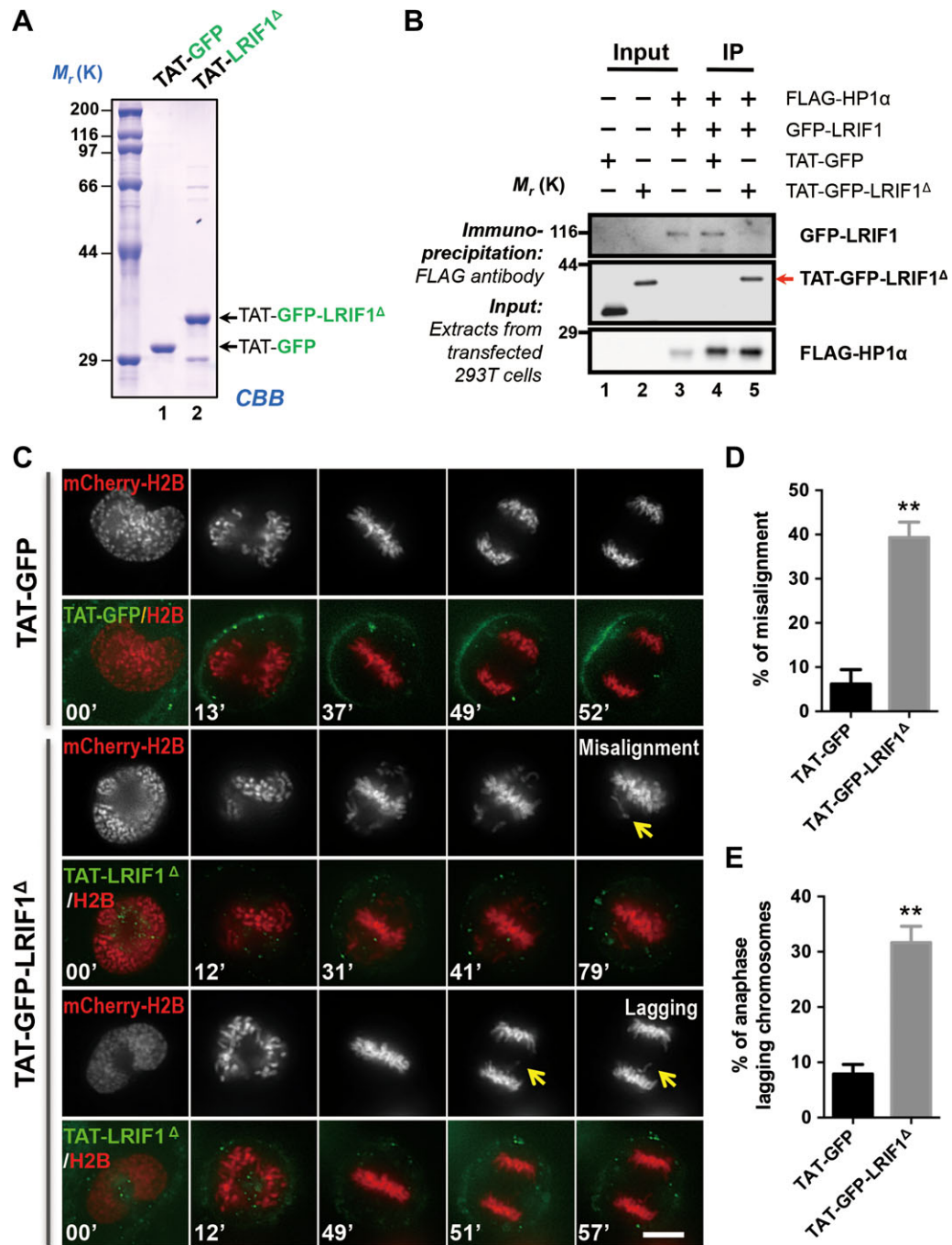


**Figure 5** Perturbation of LRIF1-HP1 $\alpha$  interaction compromises the accuracy of chromosome segregation. (A) CBB staining of SDS-PAGE gel showed the quality and quantities of the purified recombinant TAT-GFP and TAT-GFP-LRIF1 $\Delta$  (amino acids 565–600). (B) HeLa cells expressing FLAG-HP1 $\alpha$  and GFP-LRIF1 were subjected to immunoprecipitation (IP) with FLAG antibody in the presence of TAT-GFP or TAT-GFP-LRIF1 $\Delta$  for 4 h and immunoblotted with FLAG and GFP antibodies, respectively. Note that the endogenous HP1 $\alpha$ -LRIF1 interaction was perturbed by the addition of TAT-GFP-LRIF1 $\Delta$ . (C) HeLa cells expressing mCherry-H2B were synchronized with thymidine and released for 8 h to reach G2/M phase. Cells were cultured in DMEM with 2.5  $\mu$ M TAT-GFP (upper panels) or TAT-GFP-LRIF1 $\Delta$  (lower panels) at 37°C for 30 min before image collection. Live cell images were taken every 3 min. Note that TAT-GFP-LRIF1 $\Delta$ -treated cells failed to fulfill accurate chromosome alignment and segregation. Scale bar, 10  $\mu$ m. (D and E) Quantitative analyses of the mitotic progression as a function of LRIF1-HP1 $\alpha$  association. The accurate chromosome segregation was compromised in cells treated with TAT-GFP-LRIF1 $\Delta$  (2.5  $\mu$ M), which is comparable to what was seen in LRIF1-suppressed cells. At least 35 cells per group ( $n = 40$ , TAT-GFP;  $n = 35$ , TAT-GFP-LRIF1 $\Delta$ ) were examined from three independent experiments. Data represent mean  $\pm$  SEM and were examined with two-sided  $t$ -test. **\*\*** $P < 0.01$ .

synchronized with thymidine and then exposed to TAT-GFP or TAT-GFP-LRIF1<sup>A</sup> for 30 min before NEBD. While HeLa cells treated with TAT-GFP underwent normal mitosis, in the presence of 2.5  $\mu$ M TAT-GFP-LRIF1<sup>A</sup>, HeLa cells exhibited erroneous cell division characterized by misaligned and lagging chromosomes (Figure 5C–E). These results confirmed that perturbation of LRIF1–HP1 $\alpha$  interaction and suppression of LRIF1 caused similar defects in chromosome segregation. Thus, we conclude that the LRIF1–HP1 $\alpha$  interaction is required for faithful chromosome segregation during mitosis.

#### LRIF1 is essential for stable localization of HP1 $\alpha$ to the centromere

During mitosis, most HP1 $\alpha$  proteins are dissociated from chromosome arms due to Aurora B kinase-mediated phosphorylation of histone H3 at serine 10 (Fischle et al., 2005; Hirota et al., 2005; Chu et al., 2012; Qiu et al., 2012). We next questioned whether LRIF1 is required for the centromere recruitment of HP1 $\alpha$ . To this end, we first introduced LRIF1 siRNA into HeLa cells to suppress endogenous LRIF1 protein level and examined HP1 $\alpha$  localization. Interestingly, HP1 $\alpha$  signal at the centromere reduced after LRIF1 knockdown (Figure 6A and B), suggesting that recruitment of HP1 $\alpha$  to centromere requires LRIF1. To determine the specificity of LRIF1-dependent recruitment of HP1 $\alpha$  to the centromere, we examined the localization of other centromere components, including CENP-E, borealin, and Aurora B in LRIF1-suppressed cells. Compared with control siRNA-transfected cells, the localization of CENP-E, borealin, and Aurora B to centromere was intact in LRIF1-suppressed cells, confirming the specificity and requirement of LRIF1 for recruitment of HP1 $\alpha$  to the centromere (Supplementary Figure S5A and B). To examine whether HP1 $\alpha$  determines the localization of LRIF1, HeLa cells were transiently transfected to express HP1 $\alpha$  siRNA and scramble control followed by immunofluorescence microscopic analyses. LRIF1 localization to the centromeres was virtually unaltered in the HP1 $\alpha$ -suppressed cells, suggesting that centromeric localization of LRIF1 was not dependent on HP1 $\alpha$  in mitotic cells. As a positive control, the localization of borealin to the centromeres was abolished in the HP1 $\alpha$ -suppressed cells (Supplementary Figure S6A and B). We conclude that LRIF1 is required for the recruitment and stable localization of HP1 $\alpha$  to centromere during mitosis.

#### Discussion

In this study, we reported that LRIF1 specifies the centromere localization of HP1 $\alpha$  through its CS domain-binding motif within the C-terminus. The most prominent CS domain-binding interface is mapped to Val582 and Leu584 of LRIF1 on the basis of solid phase biochemical characterization and immunoprecipitation. The functional importance of this LRIF1–HP1 $\alpha$  interaction was demonstrated by the requirement of LRIF1 for temporal loading of HP1 $\alpha$  onto the centromere during cell division cycle. This LRIF1-dependent localization of HP1 $\alpha$  is essential for accurate chromosome segregation in mitosis. Collectively, our findings support a working model for HP1 $\alpha$  centromeric targeting during the cell cycle (Figure 6C). We reason that LRIF1 binds to

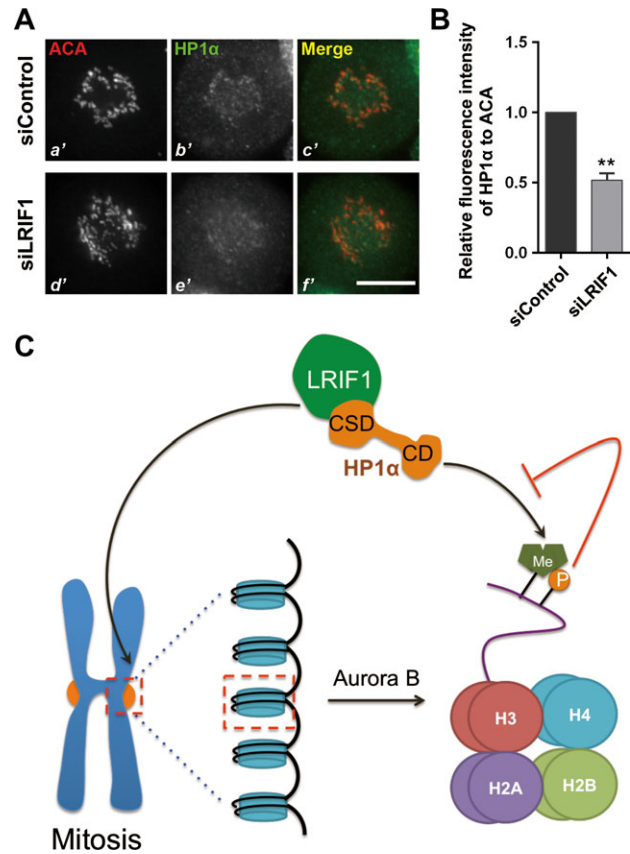


**Figure 6** LRIF1 is essential for HP1 $\alpha$  localization to the centromere. **(A)** Representative immunofluorescence images of HeLa cells transfected with control or LRIF1 siRNA for 48 h. Scale bar, 10  $\mu$ m. **(B)** Quantitative analyses of the fluorescence intensity of HP1 $\alpha$  in the centromere compared with that of ACA. A total of 100 kinetochores were examined from three independent experiments. Data represent mean  $\pm$  SEM and were examined with two-sided *t*-test. **\*\****P* < 0.01. **(C)** Model for LRIF1-mediated HP1 $\alpha$  recruitment at the centromeres during mitosis. See Discussion section for details.

CS domain of HP1 $\alpha$  through its PXXVL motif and maintains a pool of HP1 $\alpha$  at centromeres during mitosis.

Previous studies showed that different functional domains of HP1 $\alpha$  mediate its centromeric localization during interphase and mitosis (Hayakawa et al., 2003; Chu et al., 2014). In interphase, the chromodomain is required for targeting HP1 $\alpha$  to centromeres, whereas the CS domain regulates HP1 $\alpha$  localization in mitosis. Aurora B activation enables phosphorylation of its vicinity substrates to regulate multiple mitotic events essential for faithful cell division, such as biorientation and error correction (Fischle et al., 2005; Hirota et al., 2005). Also, Aurora B-dependent phosphorylation of histone H3 Ser10 during mitosis disrupts the interaction between HP1 $\alpha$  chromodomain and H3K9me2/3 (Fischle et al., 2005; Hirota et al., 2005) which leaves trace amount of HP1 $\alpha$  at the centromere. It is also reported that POGZ protein releases HP1 $\alpha$  from mitotic chromosomes by disrupting HP1 $\alpha$  binding to proteins containing PXXVL motif (Nozawa et al., 2013). Collectively, these findings suggest that centromere targeting of



HP1 $\alpha$  in mitosis likely involves multiple interactions via its CS domain with proteins containing PXVXL motif. Consistent with this notion, studies have revealed that HP1 $\alpha$  binding to the CPC subunit INCENP through its CS domain is essential for retaining the pool of HP1 $\alpha$  at centromere during mitosis (Ainsztein et al., 1998; Nozawa et al., 2010; Kang et al., 2011). Although INCENP directly recruits HP1 $\alpha$  to centromere in mitosis, cells expressing an INCENP mutant deficient for HP1 $\alpha$  binding undergo proper mitotic progression (Kang et al., 2011), which suggests that some uncharacterized centromere proteins are responsible for the residual pool of HP1 $\alpha$  at the centromere. Our present study has identified LRIF1 as a missing link that specifies the centromere localization of the HP1 $\alpha$  during mitosis through an interaction with CS domain of HP1 $\alpha$ . Cells lacking LRIF1 or with perturbed LRIF1-HP1 $\alpha$  interaction failed to conduct error-free chromosome segregation in mitosis. We reason that these multiple pathways of HP1 $\alpha$  centromere targeting are not mutually exclusive and that eukaryotic cells evolved an elaborate centromere plasticity control machinery to ensure faithful chromosome biorientation, attachment error correction, and accurate segregation in mitosis. We previously showed that TIP60 activity at the kinetochore during mitotic progress is essential for optimal Aurora B activity to prevent chromosome instability (Mo et al., 2016). It is likely the spatiotemporal dynamics of CPC distribution and precise control of Aurora B activity, priming, and activation ensure the genomic stability in mitosis through multiple pathways, including the current addressed LRIF1-HP1 $\alpha$  pathway. It is worth noting that HP1 $\alpha$  exhibits dramatic phase separation activity based on two most recent studies (Larson et al., 2017; Strom et al., 2017). The future avenue of this research will explore whether LRIF1 interaction regulates the HP1 $\alpha$  physical and biochemical properties in cell division control. It would be of great interest to uncover the mechanism of action underlying LRIF1 localization to the centromere and further elucidate how this localization is regulated during cell division cycle.

Taken together, our study demonstrates that LRIF1 specifies the localization of HP1 $\alpha$  to centromere. There are several interactive pathways underlying HP1 $\alpha$  function in prophase-to-prometaphase transition. The LRIF1-HP1 $\alpha$ -CPC hierarchical interaction model built on this study underscores the complexity of centromere protein machinery and importance of linking accurate centromere plasticity to chromosome stability during cell division cycle control.

## Materials and methods

### *Cell culture, transfection, and drug treatment*

HeLa and 293T cells from the American Type Culture Collection were maintained as subconfluent monolayers in Dulbecco's modified Eagle's medium (Gibco) with 10% fetal bovine serum (FBS; Hyclone) and 100 units/ml penicillin plus 100  $\mu$ g/ml streptomycin (Gibco) at 37°C with 8% CO<sub>2</sub>. GFP-H2B HeLa stable cell line was maintained in G418 (0.2  $\mu$ g/ $\mu$ l). HeLa cells were transfected by Lipofectamine 3000 (Invitrogen) according to the manufacturer's manual. Cells were synchronized at G1/S with 2 mM thymidine (Sigma) for 16 h, washed

with phosphate-buffered saline (PBS) three times, and then cultured in thymidine-free medium for appropriate time intervals. In some cases, HeLa cells were treated with 100 ng/ml nocodazole (Sigma) for 18 h to reach mitotic synchronization. MG132 (10  $\mu$ M) and reversine (1  $\mu$ M) were from Sigma.

### *Plasmid construction*

Human LRIF1 cDNA was obtained from the General Biosystems. Briefly, to generate GFP-tagged LRIF1, PCR-amplified cDNA was cloned into the pEGFP-C1 vector (Clontech) with *Hind*III and *Bam*HI digestion. Site-specific mutants, N-terminal (NT) or C-terminal (CT) deletion mutants of EGFP-tagged LRIF1, and RNAi-resistant LRIF1 were generated by PCR-based, site-directed mutagenesis kit from Vazyme (C212) according to the manufacturer's instructions. All plasmids used were verified by sequencing (Invitrogen). To generate TAT-GFP-LRIF1<sup>565-600</sup>-His fusion proteins, an 11-amino acid TAT sequence followed by GFP and LRIF1<sup>565-600</sup> was inserted into the pET-22b vector. TAT-GFP-His and TAT-GFP-LRIF1<sup>565-600</sup>-His fusion proteins were expressed and purified as described previously (Jiang et al., 2009).

### *Immunofluorescence and live cell imaging*

For immunofluorescence staining, HeLa cells were seeded onto sterile, acid-treated, 12-mm coverslips in 24-well plates (Corning Inc.). Cells were rinsed for 1 min with PHEM buffer (100 mM PIPES, 20 mM HEPES, pH 6.9, 5 mM EGTA, 2 mM MgCl<sub>2</sub>, and 4 M glycerol) and permeabilized for 1 min with PHEM plus 0.1% Triton X-100 (Yao et al., 2000). Extracted cells were fixed in freshly prepared 3.7% paraformaldehyde in PHEM and rinsed three times in PBS. The cells were blocked with 1% bovine serum albumin in PBS with 0.05% Tween 20 (TPBS). These cells were incubated with the various primary antibodies in a humidified chamber for 1 h at room temperature or overnight at 4°C and then washed three times in TPBS. Primary antibodies were visualized with FITC-conjugated goat anti-mouse or anti-rabbit IgG; rhodamine-conjugated goat anti-rabbit or anti-human IgG (Jackson ImmunoResearch); or Alexa Fluor 647-conjugated goat anti-human IgG (Invitrogen). DNA was stained with DAPI (Sigma).

For live cell imaging, HeLa cells expressing indicated proteins entered mitosis at 8 h after thymidine release. Transfected cells grown on glass-based dishes (MatTek) were replaced by CO<sub>2</sub>-independent medium (Gibco) supplemented with 10% FBS and observed using the DeltaVision RT system (Applied Precision) at 37°C. Images were analyzed with softWoRx software (Applied Precision).

### *Chromosome spread*

To visualize the localization of LRIF1 in metaphase chromosomes, HeLa cells were treated with nocodazole (100 ng/ml; Sigma) for 18 h followed by mitotic shaking off and collection by centrifugation. The mitotic HeLa cells were then swollen in PEM buffer (5 mM PIPES, pH 7.2, 0.5 mM EDTA, 5 mM MgCl<sub>2</sub>, 5 mM NaCl) for 10 min at room temperature. Following this, the

mitotic cells were squashed onto acid-cleaned coverslips using the cytocentrifuge (1000 rpm, 5 min), fixed and processed for immunofluorescence microscopy as previously described (Yao et al., 2000).

#### *Image acquisition and processing, fluorescence intensity quantification*

Immunofluorescence images were collected on an inverted microscope (Olympus IX-70) with a 60 $\times$ , numerical aperture 1.42 Plan Apo N objective. Step sections (0.25  $\mu$ m) were acquired to generate 3D image stacks. Olympus acquisition parameters, including exposure, focus, and illumination, were controlled by softWoRx (Applied Precision). All images for a specific experiment used identical exposure settings and scaling as described (Huang et al., 2012). The image stacks were deconvolved and projected; subsequent analysis and processing of the images were performed by softWoRx and Photoshop. All statistical analysis was performed with GraphPad Prism (GraphPad Software, Inc.).

Quantification of the levels of centromere-associated proteins was described previously (Chu et al., 2012). Briefly, the average pixel intensities within a 5  $\times$  5-pixel square positioned over a single centromere were measured, and the background pixel intensities of a 5  $\times$  5-pixel square positioned in a region of cytoplasm lacking centromeres were subtracted. Maximal projected images were used for these measurements, and the pixel intensities at each centromere pair were then normalized against ACA pixel values to account for any variations in staining or image acquisition. All of the fluorescence intensity measurements were quantified by ImageJ (National Institutes of Health).

#### *siRNA treatment, antibodies, and immunoblots*

Previously reported siRNA (Invitrogen, HSS183272) for LRIF1 (Nozawa et al., 2013) and for HP1 $\alpha$  (Dharmacon, 5'-CCUGAG AAAACUUGGAUUTT-3') (Chu et al., 2014) were used in our study. LRIF1 siRNA-2 (5'-GCUUGCUUCAUGGCCAAUTT-3') was synthesized from Genepharma. Previously described siRNA duplexes were used to repress TIP60 (Mo et al., 2016). All the siRNAs were transfected into cells using Lipofectamine 3000 for 48 h, and the knockdown efficiency was confirmed by western blotting analysis and/or immunofluorescence. Immunoblots and immunofluorescence experiments were performed with the following antibodies: anti- $\alpha$ -tubulin mouse antibody (DM1A, Sigma-Aldrich, T9026; 1:5000), anti-GFP mouse antibody (BD Biosciences; 1:2000), anti-LRIF1 rabbit antibody (Millipore; 1:200 for immunostaining and 1:1000 for western blotting), anti-HP1 $\alpha$  rabbit antibody (Cell Signaling; 1:1000 for western blotting), ACA (1:4000), anti-cyclin B1 (BD, 554177; 1:1000), anti-Mad1 (Santa Cruz, 117-468; 1:100), anti-HP1 $\alpha$  mouse antibody (ThermoFisher Scientific, 730019; 1:100 for immunostaining), and anti-Hec1 (Abcam, 9G3; 1:200). Anti-FLAG-tag antibody (M2, 1:2000) was from Sigma. For western blot experiments, equal amounts of protein from each transfected cell lysate were

heated in SDS sample buffer at 95°C for 5 min, separated by SDS-PAGE, and immunoblotted with indicated antibodies.

#### *Purification of recombinant TAT-GFP proteins and interrogation of HP1 $\alpha$ -LRIF1 in vivo*

To directly assess the functional effect of the HP1 $\alpha$ -LRIF1 interaction in mitosis, a membrane-permeable peptide containing LRIF1 amino acids 565–600 (LRIF1 <sup>$\Delta$</sup> ) was constructed as previously described (Adams et al., 2016). Briefly, this was achieved by introducing an 11-amino acid peptide derived from the TAT protein transduction domain into a fusion protein containing amino acids involving binding interface between LRIF1 and HP1 $\alpha$ . Trial experiments were employed to determine the optimal concentration to perturb HP1 $\alpha$ -LRIF1 interaction in HeLa cells, which has identified an optimal concentration of GFP-LRIF1 <sup>$\Delta$</sup>  peptide at 2.5  $\mu$ M. Purification of recombinant proteins was carried out as described previously (Huang et al., 2012). Briefly, the His-fusion proteins from bacteria in the soluble fraction were purified using Ni-NTA agarose (Qiagen). To test the efficacy of LRIF1 <sup>$\Delta$</sup>  peptide, HeLa cells expressing FLAG-HP1 $\alpha$  and GFP-LRIF1 were subjected to immunoprecipitation with FLAG antibody in the presence of TAT-GFP or TAT-GFP-LRIF1 <sup>$\Delta$</sup>  for 4 h and immunoblotted with FLAG and GFP antibodies, respectively. For introducing TAT-GFP fusion proteins to probe the functional relevance of LRIF1-HP1 $\alpha$  interaction, synchronized HeLa cells (50% confluency) were released into G2/M phase (8 h after thymidine release) before an addition of TAT-GFP peptides (2.5  $\mu$ M; TAT-GFP as control; TAT-GFP-LRIF1 <sup>$\Delta$</sup>  as disrupting peptide) at 37°C for 30 min before images collection. After incubation, the cells were washed with PBS and then examined directly under fluorescence microscopy as described previously (Ward et al., 2013).

#### *Immunoprecipitation and pull-down assays*

For immunoprecipitation, cells were treated with indicated reagents before being trypsinized and lysed in IP buffer (50 mM Tris-HCl, pH 7.9, 150 mM NaCl, 0.1% Triton X-100) supplemented with protease inhibitor cocktail (Sigma) as previously described (Liu et al., 2016). After pre-clearing with protein A/G resin, the lysate was incubated with LRIF1 antibody at 4°C for 24 h with gentle rotation. Protein A/G resin was then added to the lysates, and they were incubated for another 6 h. The Protein A/G resin was then spun down and washed five times with IP buffer before being resolved by SDS-PAGE and immunoblotted with the indicated antibodies. For FLAG-tagged protein immunoprecipitation, the FLAG-M2 resin was added to the lysates and incubated for 4 h. The binding fraction was washed with IP buffer for five times and analyzed by western blot.

For pull-down assay, GST-HP1 $\alpha$ -bound Sepharose beads were used as an affinity matrix to absorb MBP-LRIF1. Briefly, purified MBP-LRIF1 FL (full-length), MBP-LRIF1 FLM (full-length with mutation of V582D and L584E), MBP-LRIF1 CT (C-terminal truncation; amino acids 542–769), MBP-LRIF1 CTM (C-terminal truncation with mutation of V582D and L584E), and MBP-LRIF1 NT

(N-terminal truncation; amino acids 1–541) were eluted from Amylose Resin (NEB) with 10 mM maltose in MBP column buffer (20 mM Tris-Cl, pH 7.4, 200 mM NaCl, 1 mM EDTA, 1 mM DTT). GST or GST-tagged HP1 $\alpha$  proteins immobilized on agarose beads were incubated with MBP-LRIF1 proteins in pull-down buffer (20 mM Tris-Cl, pH 7.4, 100 mM NaCl, 1 mM EDTA, 5% Glycerol, 1 mM DTT) containing 0.1% Triton X-100 at 4°C for 3 h. The resins were washed three times with pull-down buffer containing 0.3% Triton X-100 and once with pull-down buffer free of Triton X-100, followed by boiling in SDS-PAGE buffer. The samples were subjected to SDS-PAGE and detected by western blots.

### Supplementary material

Supplementary material is available at *Journal of Molecular Cell Biology* online.

### Acknowledgements

The authors would like to thank Drs Xuebiao Yao and Rajagopala Sridaran for critical reading. We thank all the lab members for insightful discussion during the course of this study.

### Funding

This work was financially supported by grants from the Ministry of Science and Technology of the People's Republic of China (2017YFA0503600 and 2016YFA0100500), the National Natural Science Foundation of China (31430054, 31320103904, 91313303, 31621002, 31501095, and 31671405), the Ministry of Education of the People's Republic of China (IRT\_17R102), and the US National Institutes of Health (CA164133, DK56292, and DK115812).

**Conflict of interest:** none declared.

### References

- Adams, G. Jr., Zhou, J., Wang, W., et al. (2016). The microtubule plus-end tracking protein TIP150 interacts with cactin to steer directional cell migration. *J. Biol. Chem.* *291*, 20692–20706.
- Ainsztein, A.M., Kandels-Lewis, S.E., Mackay, A.M., et al. (1998). INCENP centromere and spindle targeting: identification of essential conserved motifs and involvement of heterochromatin protein HP1. *J. Cell Biol.* *143*, 1763–1774.
- Al-Sady, B., Madhani, H.D., and Narlikar, G.J. (2013). Division of labor between the chromodomains of HP1 and Suv39 methylase enables coordination of heterochromatin spread. *Mol. Cell* *51*, 80–91.
- Baldeyron, C., Soria, G., Roche, D., et al. (2011). HP1 $\alpha$  recruitment to DNA damage by p150CAF-1 promotes homologous recombination repair. *J. Cell Biol.* *193*, 81–95.
- Ball, A.R. Jr., and Yokomori, K. (2009). Revisiting the role of heterochromatin protein 1 in DNA repair. *J. Cell Biol.* *185*, 573–575.
- Canzio, D., Liao, M., Naber, N., et al. (2013). A conformational switch in HP1 releases auto-inhibition to drive heterochromatin assembly. *Nature* *496*, 377–381.
- Champion, L., Linder, M.I., and Kutay, U. (2017). Cellular reorganization during mitotic entry. *Trends Cell Biol.* *27*, 26–41.
- Cheutin, T., McNairn, A.J., Jenuwein, T., et al. (2003). Maintenance of stable heterochromatin domains by dynamic HP1 binding. *Science* *299*, 721–725.
- Chu, L., Huo, Y., Liu, X., et al. (2014). The spatiotemporal dynamics of chromatin protein HP1 $\alpha$  is essential for accurate chromosome segregation during cell division. *J. Biol. Chem.* *289*, 26249–26262.
- Chu, L., Zhu, T., Liu, X., et al. (2012). SUV39H1 orchestrates temporal dynamics of centromeric methylation essential for faithful chromosome segregation in mitosis. *J. Mol. Cell Biol.* *4*, 331–340.
- Cleveland, D.W., Mao, Y., and Sullivan, K.F. (2003). Centromeres and kinetochores: from epigenetics to mitotic checkpoint signaling. *Cell* *112*, 407–421.
- Fang, Z., Miao, Y., Ding, X., et al. (2006). Proteomic identification and functional characterization of a novel ARF6 GTPase-activating protein, ACAP4. *Mol. Cell. Proteomics* *5*, 1437–1449.
- Fischle, W., Tseng, B.S., Dormann, H.L., et al. (2005). Regulation of HP1-chromatin binding by histone H3 methylation and phosphorylation. *Nature* *438*, 1116–1122.
- Hayakawa, T., Haraguchi, T., Masumoto, H., et al. (2003). Cell cycle behavior of human HP1 subtypes: distinct molecular domains of HP1 are required for their centromeric localization during interphase and metaphase. *J. Cell Sci.* *116*, 3327–3338.
- Higgins, J.M., and Prendergast, L. (2016). Mitotic mysteries: the case of HP1. *Dev. Cell* *36*, 477–478.
- Hirota, T., Lipp, J.J., Toh, B.H., et al. (2005). Histone H3 serine 10 phosphorylation by Aurora B causes HP1 dissociation from heterochromatin. *Nature* *438*, 1176–1180.
- Huang, Y., Wang, W., Yao, P., et al. (2012). CENP-E kinesin interacts with SKAP protein to orchestrate accurate chromosome segregation in mitosis. *J. Biol. Chem.* *287*, 1500–1509.
- Inoue, A., Hyle, J., Lechner, M.S., et al. (2008). Perturbation of HP1 localization and chromatin binding ability causes defects in sister-chromatid cohesion. *Mutat. Res.* *657*, 48–55.
- Jiang, K., Wang, J., Liu, J., et al. (2009). TIP150 interacts with and targets MCAK at the microtubule plus ends. *EMBO Rep.* *10*, 857–865.
- Juang, B.T., Gu, C., Starnes, L., et al. (2013). Endogenous nuclear RNAi mediates behavioral adaptation to odor. *Cell* *154*, 1010–1022.
- Kang, J., Chaudhary, J., Dong, H., et al. (2011). Mitotic centromeric targeting of HP1 and its binding to Sgo1 are dispensable for sister-chromatid cohesion in human cells. *Mol. Biol. Cell* *22*, 1181–1190.
- Kiyomitsu, T., Iwasaki, O., Obuse, C., et al. (2010). Inner centromere formation requires hMis14, a trident kinetochore protein that specifically recruits HP1 to human chromosomes. *J. Cell Biol.* *188*, 791–807.
- Kwon, S.H., Florens, L., Swanson, S.K., et al. (2010). Heterochromatin protein 1 (HP1) connects the FACT histone chaperone complex to the phosphorylated CTD of RNA polymerase II. *Genes Dev.* *24*, 2133–2145.
- Larson, A.G., Elnatan, D., Keenen, M.M., et al. (2017). Liquid droplet formation by HP1 $\alpha$  suggests a role for phase separation in heterochromatin. *Nature* *547*, 236–240.
- Li, H.J., Haque, Z.K., Chen, A., et al. (2007). RIF-1, a novel nuclear receptor corepressor that associates with the nuclear matrix. *J. Cell. Biochem.* *102*, 1021–1035.
- Liu, D., Liu, X., Zhou, T., et al. (2016). IRE1-RACK1 axis orchestrates ER stress preconditioning-elicited cytoprotection from ischemia/reperfusion injury in liver. *J. Mol. Cell Biol.* *8*, 144–156.
- Liu, X., Song, Z., Huo, Y., et al. (2014). Chromatin protein HP1 interacts with the mitotic regulator borealin protein and specifies the centromere localization of the chromosomal passenger complex. *J. Biol. Chem.* *289*, 20638–20649.
- Luijsterburg, M.S., Dinant, C., Lans, H., et al. (2009). Heterochromatin protein 1 is recruited to various types of DNA damage. *J. Cell Biol.* *185*, 577–586.
- Mo, F., Zhuang, X., Liu, X., et al. (2016). Acetylation of Aurora B by TIP60 ensures accurate chromosomal segregation. *Nat. Chem. Biol.* *12*, 226–232.
- Nonaka, N., Kitajima, T., Yokobayashi, S., et al. (2002). Recruitment of cohesin to heterochromatic regions by Swi6/HP1 in fission yeast. *Nat. Cell Biol.* *4*, 89–93.
- Nozawa, R.S., Nagao, K., Igami, K.T., et al. (2013). Human inactive X chromosome is compacted through a PRC2-independent SMCHD1-HiX1 pathway. *Nat. Struct. Mol. Biol.* *20*, 566–573.
- Nozawa, R.S., Nagao, K., Masuda, H.T., et al. (2010). Human POGZ modulates dissociation of HP1 $\alpha$  from mitotic chromosome arms through Aurora B activation. *Nat. Cell Biol.* *12*, 719–727.

- Obuse, C., Iwasaki, O., Kiyomitsu, T., et al. (2004). A conserved Mis12 centromere complex is linked to heterochromatic HP1 and outer kinetochore protein Zwint-1. *Nat. Cell Biol.* 6, 1135–1141.
- Patel, H., Stavrou, I., Shrestha, R.L., et al. (2016). Kindlin1 regulates microtubule function to ensure normal mitosis. *J. Mol. Cell Biol.* 8, 338–348.
- Qiu, Y., Liu, L., Zhao, C., et al. (2012). Combinatorial readout of unmodified H3R2 and acetylated H3K14 by the tandem PHD finger of MOZ reveals a regulatory mechanism for HOXA9 transcription. *Genes Dev.* 26, 1376–1391.
- Rajagopalan, H., and Lengauer, C. (2004). Aneuploidy and cancer. *Nature* 432, 338–341.
- Rougemaille, M., Braun, S., Coyle, S., et al. (2012). Ers1 links HP1 to RNAi. *Proc. Natl Acad. Sci. USA* 109, 11258–11263.
- Shen, Z. (2011). Genomic instability and cancer: an introduction. *J. Mol. Cell Biol.* 3, 1–3.
- Shimura, M., Toyoda, Y., Iijima, K., et al. (2011). Epigenetic displacement of HP1 from heterochromatin by HIV-1 Vpr causes premature sister chromatid separation. *J. Cell Biol.* 194, 721–735.
- Strom, A.R., Emelyanov, A.V., Mir, M., et al. (2017). Phase separation drives heterochromatin domain formation. *Nature* 547, 241–245.
- Studencka, M., Wesolowski, R., Opitz, L., et al. (2012). Transcriptional repression of Hox genes by *C. elegans* HP1/HPL and H1/HIS-24. *PLoS Genet.* 8, e1002940.
- Verschure, P.J., van der Kraan, I., de Leeuw, W., et al. (2005). In vivo HP1 targeting causes large-scale chromatin condensation and enhanced histone lysine methylation. *Mol. Cell Biol.* 25, 4552–4564.
- Ward, T., Wang, M., Liu, X., et al. (2013). Regulation of a dynamic interaction between two microtubule-binding proteins, EB1 and TIP150, by the mitotic p300/CBP-associated factor (PCAF) orchestrates kinetochore microtubule plasticity and chromosome stability during mitosis. *J. Biol. Chem.* 288, 15771–15785.
- Yamagishi, Y., Sakuno, T., Shimura, M., et al. (2008). Heterochromatin links to centromeric protection by recruiting shugoshin. *Nature* 455, 251–255.
- Yao, X., Abrieu, A., Zheng, Y., et al. (2000). CENP-E forms a link between attachment of spindle microtubules to kinetochores and the mitotic checkpoint. *Nat. Cell Biol.* 2, 484–491.